CHEMISTRY
A EUROPEAN JOURNAL

DOI: 10.1002/chem.200902405

A Doppel α-Helix Peptide Fragment Mimics the Copper(II) Interactions with the Whole Protein

Diego La Mendola,[b] Antonio Magrì,[b] Tiziana Campagna,[b] Maria Anna Campitiello,[c] Luca Raiola,[c, f] Carla Isernia,[c] Örjan Hansson,[d] Raffaele P. Bonomo,[a] and Enrico Rizzarelli*[a, e]

Abstract: The doppel protein (Dpl) is the first homologue of the prion protein (PrP^C) to be discovered; it is overexpressed in transgenic mice that lack the prion gene, resulting in neurotoxicity. The whole prion protein is able to inhibit Dpl neurotoxicity, and its N-terminal domain is the determinant part of the protein function. This region represents the main copper(II) binding site of PrP^C. Dpl is able to bind at least one copper ion, and the specific metal-binding site has been identified as the histidine residue at the beginning of the third helical region. However, a reliable characterization of copper(II) coordination features has not been reported. In a previous paper, we studied the copper(II) interaction with a peptide that encompasses only the loop region potentially involved in metal binding. Nevertheless, we did not find a complete match between the EPR spectroscopic parameters of the copper(II) complexes formed with the synthesized peptide and those reported for the copper(II) binding sites of the whole protein. Herein, the synthesis of the human Dpl peptide fragment hDpl-(122–139) (Ac-KPDNKLHQQVLWR-LVQEL-NH_2) and its copper(II) complex species are reported. This peptide encompasses the third α helix and part of the loop linking the second and the third helix of human doppel protein. The single-point-mutated peptide, hDpl(122–139)D124N, in which aspartate 124 replaces an asparagine residue, was also synthesized. This peptide was used to highlight the role of the carboxylate group on both the conformation preference of the Dpl fragment and its copper(II) coordination features. NMR spectroscopic measurements show that the hDpl(122–139) peptide fragment is in the prevailing α-helix conformation. It is localized within the 127–137 amino acid residue region that represents a reliable conformational mimic of the related protein domain. A comparison with the single-point-mutated hDpl(122–139)D124N reveals the significant role played by the aspartic residue in addressing the peptide conformation towards a helical structure. It is further confirmed by CD measurements. Potentiometric titrations were carried out in aqueous solutions to obtain the stability constant values of the species formed by copper(II) with the hDpl peptides. Spectroscopic studies (EPR, NMR, CD, UV/Vis) were performed to characterize the coordination environments of the different metal complexes. The EPR parameters of the copper(II) complexes with hDpl(122–139) match those of the previously reported copper(II) binding sites of the whole hDpl. Addition of the copper(II) ion to the peptide fragment does not alter the helical conformation of hDpl(122–139), as shown by CD spectra in the far-UV region. The aspartate-driven preorganized secondary structure is not significantly modified by the involvement of Asp124 in the copper(II) complex species that form in the physiological pH range. To elaborate on the potential role of copper(II) in the recently reported interaction between the PrP^C and Dpl, the affinity of the copper(II) complexes towards the prion N terminus domain and the binding site of Dpl was reported.

Keywords: copper · doppel proteins · helical structures · peptides · prions

[a] Prof. R. P. Bonomo, Prof. E. Rizzarelli
Dipartimento di Scienze Chimiche
Università degli Studi di Catania
Viale A. Doria 6, 95125 Catania (Italy)
Fax: (+39) 095337678
E-mail: erizzarelli@unict.it

[b] Dr. D. La Mendola, Dr. A. Magrì, T. Campagna
Istituto di Biostrutture e Bioimmagini-CNR
c/o Dipartimento di Scienze Chimiche
Viale A. Doria 6, 95125 Catania (Italy)

Introduction

The doppel protein is mainly expressed in the reproductive system, more specifically in Sertoli cells and spermatozoa, and only in a minimal amount in the central nervous system.[1,2] The exact biological function is still unclear, but its deregulation causes male sterility.[3] The protein is encoded by a gene located 16–20 kb downstream from that of the prion protein (PrP^C), and is usually abbreviated to Dpl (downstream prion protein-like).[4,5] Interestingly, an N-terminal truncated form of PrP^C is the most prominent prion species in the testes, which suggests that the C-terminal domain of prion and Dpl might have a similar biological function within the reproductive system.[6]

Dpl and the structured domain of PrP^C share only about 25% in the identity of their primary sequences; despite this, they show a very similar three-dimensional structure composed of three α helices and two short β strands.[7] However, Dpl has an additional disulfide bridge and does not contain the tandem repeat region and hydrophobic core that are present in PrP^C of different species. Dpl does not seem to be directly involved in prion disease, but it is neurotoxic when overexpressed in the brain of mice deprived of PrP^C.[2,8–10] It is interesting to point out that Dpl toxicity effects are very similar to those determined by PrP^C lacking the N-terminal domain, and in both cases its toxicity is inhibited by the full-length PrP^C protein when PrP^c is either endogenously expressed or exogenously applied.[9–13] In this respect, the PrP^C N-terminal region appears to be necessary for this function, even if contrasting results have been reported.[12–14] Doppel was initially identified as a prion-like protein due to its structural and biochemical similarities to prion protein (PrP^C), but emerging evidence now suggests that the function of prion proteins is more antagonistic to doppel than synergistic, though a plausible molecular mechanism for their biological antagonism is lacking. The formation of a multimeric complex between Dpl and PrP^C has been hypothesized,[12] and interaction or direct competition with a common ligand partner or a cofactor, such as a metal ion, have also been suggested.[15]

Many lines of evidence indicate that PrP^C is a copper-binding protein in vivo, and its biological role might be strictly connected with copper homeostasis.[16,17] The N-terminal domain of prion protein, with its octarepeats and hydrophobic domain, is thought to be the main copper-binding domain, and it can bind up to five or six metal ions.[18] Despite the absence of an analogous copper(II)-binding PrP^C region, Dpl binds at least one metal equivalent.[19–21] The specific copper(II) binding site has been localized at histidine residues 131 and 128 in the mouse and human sequences, respectively, within the loop included between the second and the third helical region.[19,20] CD spectra have shown an enhancement of the α-helical content of whole human doppel (hDpl) protein after copper addition,[20] whereas the metal ion did not modify the CD spectra of mouse doppel (mDpl) protein.[19] Equilibrium dialysis and fluorescence-quenching analysis have been carried out to estimate the affinity constant values of the copper(II)–mDpl complexes.[19] EPR spectroscopic parameters have been attributed to different copper(II) binding sites in hDpl as a function of pH.[20]

To associate the different coordination environments with the single copper(II) complex species, we recently reported a detailed study on the copper(II) interactions with both hDpl(122–130) (Ac-KPDNKLHQQ-NH_2), a peptide encompassing the loop region potentially involved in copper(II) binding, and its single-point-mutated peptide in which the aspartate residue has been substituted by an asparagine.[22] A comparison of the EPR spectroscopic parameters obtained for these copper(II) complexes with those reported for the whole hDpl provided a partial description of the copper(II) coordination environments of the different complex species formed by changing the pH values. Thus, being aware that the histidine, acts as anchor site for copper(II) and is located at the beginning of the third α-helical region, we herein extend our previous investigation to the longer peptide fragment hDpl(122–139) (Ac-KPDNKLHQQVLW-RLVQEL-NH_2) as a better mimic molecule of the hDpl binding domain. This new peptide encompasses sequence 122–139, which contains both the third α helix and part of the loop that links the second and the third helix of hDpl (Figure 1).

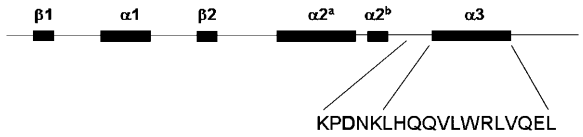

hDpl(122-139) = KP**D**NKLHQQVLWRLVQEL
hDpl(122-139)D124N = KP**N**NKLHQQVLWRLVQEL

Figure 1. Schematic view of the doppel protein secondary structure and the primary sequences of hDpl(122–139) and hDpl(122–139)D124N.

[c] Dr. M. A. Campitiello, Dr. L. Raiola, Prof. C. Isernia
Dipartimento di Scienze Ambientali
Seconda Università di Napoli
Via A. Vivaldi 43, 81100 Caserta (Italy)

[d] Prof. Ö. Hansson
Department of Chemistry
University of Gothenburg, PO Box 462
SE-405 30 Gothenburg (Sweden)

[e] Prof. E. Rizzarelli
Istituto Nazionale di Biostrutture e Biosistemi
Consorzio Interuniversitario
Viale Medaglie d'oro 305, 00136 Roma (Italy)

[f] Dr. L. Raiola
Present address: Département de Biochimie, Université de Montréal
C.P. 6128 Succursale Centre-Ville
Montréal, QC, H3C 3J7 (Canada)

Supporting information for this article is available on the WWW under http://dx.doi.org/10.1002/chem.200902405.

NMR spectroscopy measurements were carried out to determine the conformational features of the hDpl(122–139) peptide fragment, whereas a combined potentiometric and spectroscopic approach (EPR, CD, UV/Vis) was used to obtain the affinity constants, the species distribution as a function of pH, and the coordination environments of copper(II) complexes. NMR and CD spectroscopic measurements of the copper(II) complexes were also performed to shed light onto the conformational changes induced by copper(II) addition on the secondary structure of the hDpl fragment. Analogously to our previous paper,[22] we have also synthesized a single-point-mutated peptide, hDpl(122–139)D124N, in which the aspartate amino acid has been substituted by an asparagine residue, to unveil the role of the carboxylate group on the copper(II) coordination features. The role of the preorganized system present in hDpl(122–139) was obtained by comparing its thermodynamic and spectroscopic data with those of the shorter and unstructured hDpl(122–130).

Results and Discussion

Determining the secondary structures of hDpl(122–139) and hDpl(122–139)D124N by using NMR and CD spectroscopy: Proton chemical shifts, ^3J(HN,Hα) scalar coupling, and $\Delta\delta/\Delta T$ at pH 4.0 for hDpl(122–139) and hDpl(122–139)D124N have been submitted to the Biological Magnetic Resonance Data Bank (BMRB). The chemical shift of hDpl(122–139) and hDpl(122–139)D124N are reported in Table 1S and 2S, respectively (see the Supporting Information). The NOE connectivity diagrams for hDpl(122–139) and hDpl(122–139)D124N are reported in Figure 2.

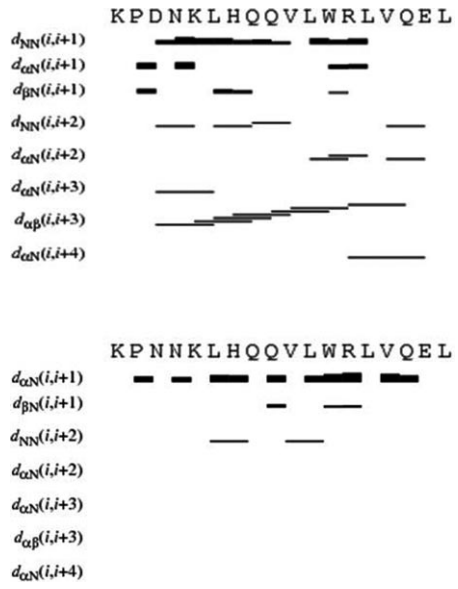

Figure 2. Sequential and medium-range NOE connectivities observed in aqueous solution at pH 4.0 for A) hDpl(122–139) and B) hDpl(122–139)D124N.

The NOE diagrams show strong differences between the investigated peptides; in particular, a typical pattern of helicoidal secondary-structure NOEs is observed for hDpl(122–139). This behavior was confirmed by the temperature coefficients of the backbone amide protons. In fact, temperature gradients showed different trends for the two molecules: in the wild-type peptide, the temperature coefficients had lower values than those observed for the same residues in the mutant.

A total of 308 NOEs (142 interresidues, 166 intraresidues) were obtained for hDpl(122–139) from the NOESY 250 ms spectrum; these NOEs, together with 15 ^3J(HN,Hα) scalar coupling constants resulted in 252 meaningful distance constraints and 94 angle constraints, which were used for the structure calculations. 194 ROEs (26 interresidues, 168 intraresidues, ROESY mixing time: 150 ms), 17 ^3J(NH,Hα) coupling constants, 96 meaningful distance constraints, and 96 angle constraints were obtained and used in the structure determination of hDpl(122–139)D124N.

All the constraints were used to generate a total of 100 structures, and among them the 20 with the lowest target function were selected and energy minimized. The obtained structures satisfied the NMR spectroscopic constraints, with no NOE violations greater than 0.2 Å. In Figure 3, the superimposition of the 20 minimized structures is reported for hDpl(122–139) and hDpl(122–139)D124N whereas in Figure 1S in the Supporting Information the corresponding conformers are shown. Average backbone dihedral angles are listed in Table 3S, and hydrogen bond distances and angles are in Table 4S.

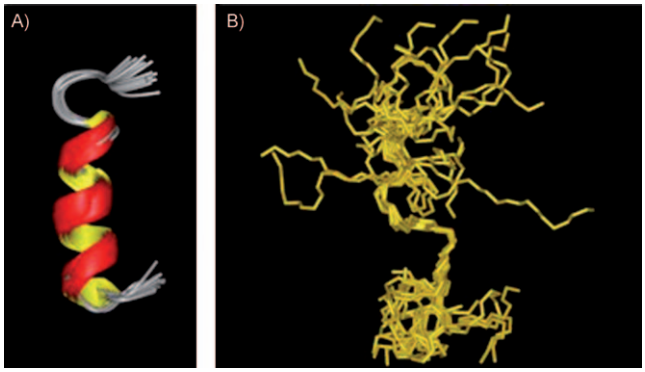

Figure 3. Superposition of the 20 lowest energy CYANA conformers of A) hDpl(122–139) and B) hDpl(122–139)D124N in H_2O. The structures were minimized in vacuo and aligned according to the minimal RMSD of the backbone atom residues. Only the polypeptide backbone is shown (top: N terminus, bottom; C terminus).

The hDpl(122–139) peptide fragment exhibits an extensive defined helical region, with a root-mean-square deviation (RMSD) from the mean structure of 0.42 Å for the L127–Q137 region, and disordered N- and C-terminal tails. The main structured part is an α helix that spans residues Q130–Q137, with mean values of ϕ and ψ angles of −64 and −39°, respectively; the structure is stabilized by three (i, $i+$

4) hydrogen bonds. Residues L127–Q129 exhibit typical 3_{10} helix ϕ and ψ angles in 40% of the minimized structures.

Not all of the calculated structures of hDpl(122–139)D124N converge to a defined conformation even if a discrete superimposition was found for the backbone region Q129–L135 (RMSD = 0.70 Å); the results are those expected considering the low number of recorded NOE and ROE effects.

A complete NMR spectroscopic analysis was also performed in water at pH 5.5 for both peptides prior to copper(II) titrations. The recorded NMR spectroscopy parameters and structure calculation data confirmed the results obtained at dissolution pH; this reinforces the assumption of a helical conformation in the L127–Q137 region in the hDpl-(122–139) case.

The NMR spectroscopic analysis demonstrates that sequence 127–137 of the hDpl(122–139) peptide effectively maintains its helical nature even if it is excised from the whole hDpl protein. Actually, a comparison of the chemical shifts measured for the α-amino acid residues of the hDpl-(122–139) peptide fragment with those reported for the same sequence of the full-length protein reveals some differences in terms of helical conformation percentage.[7] However, these differences can be easily explained by considering that sequence 122–139 in the protein is also subjected to long-range interactions determined by its tertiary structure. In any case, the NMR spectroscopy results indicate that the hDpl(122–139) peptide fragment represents a suitable model for the study of copper-(II) interactions within the α-3 helix of the full-length protein (Figure 4).

Figure 4. Superposition of the whole hDpl structure (red/yellow; as reported in the PDB (ID 1LG4))[7] and a representative hDpl(122–139) conformer (blue); backbone atoms of residues from Leu127 to Gln137 were superimposed (RMSD 1.4 Å).

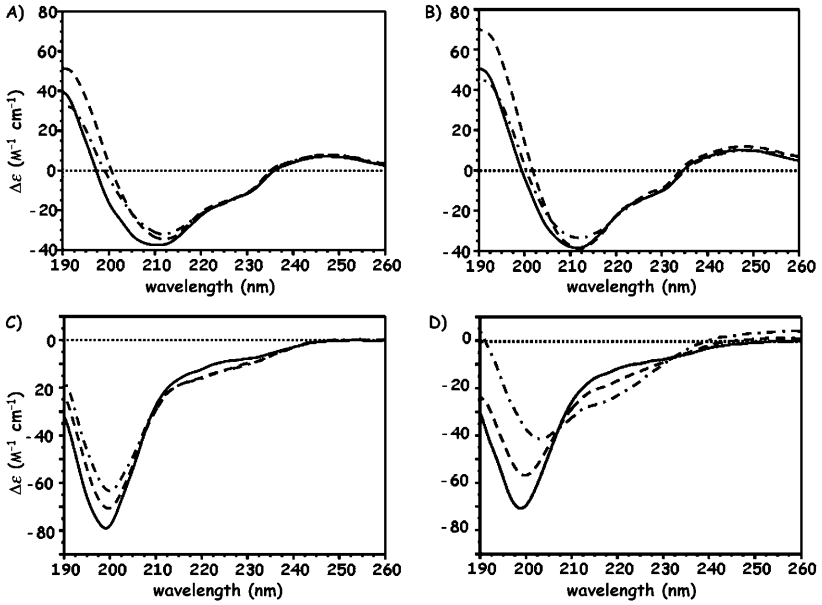

Figure 5. CD spectra of A) hDpl(122–139), B) Cu–hDpl(122–139), C) hDpl(122–139)D124N, and D) Cu–hDpl-(122–139)D124N recorded in H_2O at pH 4 (——), 7 (– – –), and 9 (–•–•). $[L] = 5 \times 10^{-6}$ mol dm^{-3}, M/L molar ratio 1:1.

The CD spectra of hDpl(122–139) show a maximum around $\lambda = 192$ nm, a minimum at $\lambda = 210$ nm, a shoulder around $\lambda = 220$ and a positive band centered around $\lambda = 250$ nm (Figure 5A). The band shape is similar to that observed for other peptides with a substantial α-helical content;[23] the deconvolution of the spectra, carried out by using the CDNN software,[24] gives a high α-helical content (roughly 90%) at pH values of between 4 and 10. The wide band centered around $\lambda = 250$ nm can be attributed to the indole group of the tryptophan residue by taking into account the contribution of aromatic side-chains to the near-UV CD spectra.[25] The presence of a signal in this region is a further indication of the presence of structured conformations because the intensity of this transition is tuned by the electronic environment determined by the rest of the molecule, CD bands produced by flexible conformations give rise to very small signals.[26] Unlike hDpl(122–139), the CD spectrum of its mutated analogue at pH 4 is dominated by a strong negative band at $\lambda = 199$ nm, which is typical of a random coil conformation (Figure 5C). The deconvolution of the spectra by using the CDNN software[24] confirms the high random coil content in

the pH range investigated. These results are also in keeping with the NMR spectroscopy data.

The influence of copper(II) on hDpl(122–139) and hDpl-(122–139)D124N conformation: The interaction between copper(II) and hDpl(122–139) does not significantly affect the essential spectral features (Figure 5B). Only a slight increase in the intensity of the positive peak at $\lambda = 192$ nm is observed at basic pH values; the other two bands at $\lambda = 210$ and 250 nm are almost unaffected by the presence of copper(II). These data suggest that addition of copper ions does not affect the secondary structure of peptide, although the contribution of metal-induced charge-transfer bands cannot be excluded. In contrast, the addition of copper(II) to hDpl-(122–139)D124N induces significant changes in the CD spectra at pH values greater than 6 (Figure 5D). A clear decrease in the minimum intensity along with a redshift towards $\lambda = 203$ nm was observed, accompanied by an enhancement of the negative ellipticity around $\lambda = 220$ nm. The difference spectra, obtained by subtracting the parent ligand CD spectra from those obtained after copper(II) addition, suggest an increase in turn conformation driven by copper(II) complex formation (data not shown). Similar structuring effects within the polypeptide backbone have been reported for the shorter doppel peptide fragments previously studied and have been explained by taking into account the involvement of the deprotonated amide nitrogen atoms in the copper(II) binding.[22]

Previously reported copper(II) binding sites of whole doppel protein and hDpl(122–139)copper(II) complexes: The pK_{lh} values of hDpl(122–139) and hDpl(122–139)D124N, obtained by means of potentiometric measurements, are reported in Table 1. The two protonation equilibria of the aspartic and glutamic acid residues in hDpl(122–139) overlap significantly; the comparison with the pK_{lh} value of glutamic acid residue of hDpl(122–139)D124N suggests that the lowest pK_{lh} value belongs to the aspartic acid residue. This hypothesis is in agreement with the general finding that aspartic β-carboxylic groups are more acidic than glutamic γ-carboxylic groups.[27,28] The pK_{lh} values of the imidazole side-chain are identical in the two peptides, and both correspond well with those of other histidine-containing ligands.[29] The other pK_{lh} values of hDpl(122–139) and hDpl(122–139)D124N are due to the deprotonation of the two lysine residues. It is worth noting that the difference between the pK_{lh} values of the lysine residues in hDpl(122–139) ($\Delta pK_{lh} = 0.78$) is larger than that observed in hDpl-(122–139)D124N ($\Delta pK_{lh} = 0.33$) and its shorter Dpl peptide fragment 122–130 ($\Delta pK_{lh} = 0.56$[22]). If the relatively low pK_{lh} value of the aspartate carboxylic group is also taken into account, an electrostatic interaction between the aspartic carboxyl group and amino group of lysine residues that might cause or be related to the structured conformation of hDpl-(122–139) can be hypothesized, in comparison with the random coil conformation of hDpl(122–139)D124N.

Table 1. Stability constant values (logβ) of proton and copper(II) complexes of hDpl(122–139) and hDpl(122–139)D124N ($T = 298$ K, $KNO_3 = 0.1$ mol dm^{-3}).[a]

Species	hDpl(122–139)[b]	Species	hDpl(122–139)D124N[b]
LH_5^{3+}	32.81(3)		
LH_4^{2+}	30.12(2)	LH_4^{3+}	29.77(3)
LH_3^{+}	27.19(2)	LH_3^{2+}	26.94(2)
LH_2	20.94(2)	LH_2^{+}	20.65(2)
LH^{-1}	10.86(3)	LH	10.49(2)
pK(Asp)	2.69		
pK(Glu)	2.93	pK(Glu)	2.83
pK(His)	6.25	pK(His)	6.29
pK(Lys$_1$)	10.08	pK(Lys$_1$)	10.16
pK(Lys$_2$)	10.86	pK(Lys$_2$)	10.49
$[CuLH_2]^{2+}$	25.05(8)		
$[CuLH]^{+}$	19.61(4)	$[CuLH]^{2+}$	17.83(4)
[CuL]	12.04(8)	$[CuL]^{+}$	11.33(2)
$[CuLH_{-1}]^{-1}$	4.87(5)	$[CuLH_{-1}]$	3.01(4)
$[CuLH_{-2}]^{-2}$	−4.54(8)	$[CuLH_{-2}]^{-1}$	−6.98(5)
$[CuLH_{-3}]^{-3}$	−14.41(6)	$[CuLH_{-3}]^{-2}$	−17.84(5)

[a] $pK_{lh} = \log\beta_{lh} - \log\beta_{l(h-1)}$. [b] σ in parentheses.

The investigated doppel peptide fragments contain a single histidine anchoring site for copper ions, and even if high metal-to-ligand molar ratios were used, only mononuclear copper(II) complexes were found. As previously observed for the shorter peptide fragment,[22] peptide hDpl-(122–139) starts to coordinate at pH values lower than the single-point-mutated analogue (see Figure 6).

The first metal complex formed by hDpl(122–139) is $[CuLH_2]^{2+}$: the equilibrium reaction $Cu^{2+} + H_2L \rightleftarrows CuLH_2^{2+}$ has a log$K$ value of 4.11, which is higher than that reported for copper(II) bound to only one imidazole nitrogen atom;[29] this indicates the additional involvement of the aspartic carboxylate group in the copper(II) coordination environment. UV/Vis parameters are listed in Table 2; the λ_{max} (705 nm) and ε (50 mol dm^{-3} cm^{-1}) values support this coordination mode. The EPR spectroscopy parameters (Table 2) are very similar to those obtained for the copper(II) complex with the shorter peptide hDpl(122–130) and the whole protein at acidic pH values (D1: $g_{\parallel} = 2.320$ and $A_{\parallel} = 163 \times 10^{-4}$ cm^{-1};[20] see ref. [20] for more infrmation).

The absence of an analogous copper complex species for hDpl(122–139)D124N (see Figure 6, bottom) again indicates the involvement of the aspartate carboxylic group in the native hDpl(122–139) binding to copper(II). However, NMR spectroscopic measurements of both peptides after copper(II) addition have been carried out, and provide further evidence of the copper(II) coordination mode. Diffusion NMR spectroscopy experiments were recorded at pH 5.5 in the absence and presence of the metal ion to exploit the stoichiometry of copper(II) complexes and the amino acid residues involved in the binding. The translational diffusion coefficient, D_{trans}, measured on the peptides gave values of $2.05 \pm 0.05 \times 10^{-10}$ and $1.96 \pm 0.05 \times 10^{-10}$ m^2 s^{-1} for hDpl(122–139) and hDpl(122–139)D124N, respectively; both correspond to a calculated average molecular size of about 2400 Da.[30] D_{trans} assumed similar average values when different aliquots of Cu^{2+} were added to the samples,

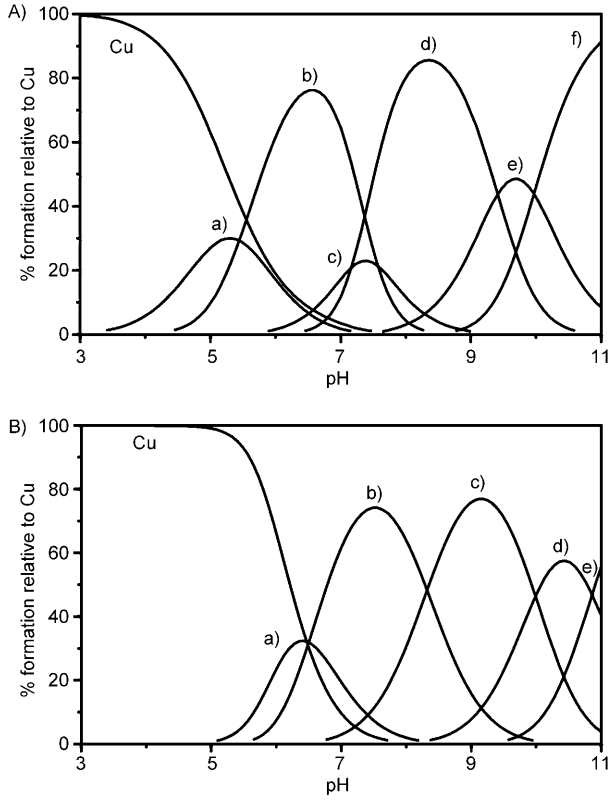

Figure 6. Species distribution diagram for Cu^{II} complexes of hDpl(122–139) (top) and hDpl(122–139)D124N ligands (bottom) in aqueous solution. a) $[CuLH_2]$; b) [CuLH]; c) [CuL]; d) $[CuLH_{-1}]$; e) $[CuLH_{-2}]$; f) $[CuLH_{-3}]$. Charges are omitted for clarity. $[L]=1\times10^{-3}$ mol dm^{-3}, M/L molar ratio 1:1.

which leads to the conclusion that no peptide–peptide aggregation occurs in the investigated ratios of hDpl(122–139) and hDpl(122–139)D124N to copper(II). The addition of $CuSO_4$ to hDpl(122–139) and hDpl(122–139)D124N caused differential broadening of the resonances. The affected residues were identified by comparing their intensities (I) with those of the same peak (I_0) observed in the absence of Cu^{2+}; I/I_0 ratios of nonoverlapping protons are reported in Figure 7 as a function of the peptide sequence. In particular, we found that Asp124 and His128 β-proton resonances in hDpl(122–139) completely vanished in the presence of 0.3 equivalents of the paramagnetic ion. His128 H_β signals were also substantially affected by the Cu^{2+} addition to hDpl(122–139)D124N. In both cases, the aromatic His128 H_δ showed the same trend as H_β, whereas the H_ε behavior could not be monitored because each peak was overlapped with the proper HN resonance.

On the whole, the data obtained for the $[CuLH_2]^{2+}$ strongly support a 1N3O set of donor atoms (N_{Im}, COO^- Asp, $2H_2O$) in the analogous copper(II) complex with the whole doppel protein at acidic pH (the D1 species previously reported[20]). It is interesting to note that hDpl(122–139) forms the $[CuLH_2]^{2+}$ complex species in a lower amount than the shorter, unordered peptide hDpl(122–130). In fact, this complex species is the prevailing one only up to pH 5.2.

In striking contrast to the hDpl(122–130) peptide, $[CuLH]^+$ is the major species in the pH range of 5.5 to 7.4. The pK_{lh} value ($pK_{lh}=5.44$) is related to the deprotonation of an amide nitrogen atom with the two lysine amino groups still protonated ($[CuLH]^+=[CuL_{-1}(H_2)]^+$). The logβ value observed for $[CuLH]^+$ of hDpl(122–139) is 1.8 log units higher than the corresponding copper(II) complex with hDpl(122–139)D124N, a difference caused by the involvement of the carboxylate group in the copper(II) coordination and also in the $[CuLH]^+$ complex species. Therefore, copper(II) is bound to one imidazole and one amide nitrogen atom, and an oxygen atom from the carboxylate group of the aspartic residue; this coordination environment might also be favored by the preorganized structure of hDpl(122–139). Accordingly, the logβ value of $[CuLH]^{2+}$ for hDpl(122–139)D124N is similar to that reported for the shorter peptide fragments[22] that analogously showed a random coil conformation. The UV/Vis and CD spectroscopy parameters confirm a 2N2O (N_{Im}, N^-, $2H_2O$) in-plane coordination mode. The presence of a band at $\lambda=$ 345 nm and a shoulder around

Table 2. Spectroscopic parameters of copper(II) complexes of hDpl(122–139) and hDpl(122–139)D124N. $[Cu]=[L]=1\times10^{-3}$ mol dm^{-3}.

Species	UV/Vis		CD		EPR[a]	
	λ [nm]	ε [mol dm^{-3} cm^{-1}]	λ [nm]	$\Delta\varepsilon$ [mol dm^{-3} cm^{-1}]	$g_\parallel$	$A_\parallel$ [10^4 cm^{-1}]
L=hDpl(122–139)						
$[CuLH_2]^{2+}$	705	50	360, 718	−0.016, +0.028	2.320(2)	165(3)
$[CuLH]^+$	650	70	303 sh, 350, 478, 550, 723	+0.165, −0.110, −0.112, +0.084, −0.112	2.275(2)	175(3)
[CuL]	–	–	–	–	2.264(3)	182(5)
$[CuLH_{-1}]^{-1}$	525	115	321, 365, 490, 627	+0.850, −0.090, −0.846, +0.578	2.192(2)	197(3)
$[CuLH_2]^{-2}$	525	115	322, 370, 490, 630	+0.978, −0.090, −1.080, +0.732	2.191(2)	197(3)
$[CuLH_3]^{-3}$	525	115	323, 370, 492, 628	+0170, −0.060, −1.035, +0.764	2.181(2)	198(3)
L=hDpl(122–139)D124N						
$[CuLH]^{2+}$	–	–	300 sh, 347, 418, 535, 630	+0.180, −0.112, −0.040, +0.122, −0.096	–	–
$[CuL]^+$	605	75	302 sh, 353, 478, 546, 723	+0.200, −0.176, −0.160, +0.168, −0.112	2.227(2)	172(2)
$[CuLH_{-1}]$	525	105	323, 370, 490, 629	+0.922, −0.064, −0.958, +0.653	2.190(2)	196(3)
$[CuLH_{-2}]^{-1}$ $[CuLH_{-3}]^{-2}$	525	110	323, 365, 490, 627	−0.950, −0.037, −0.930, +0.662	2.190(2)	196(3)

[a] For EPR spectroscopy data, experimental errors are reported in parentheses.

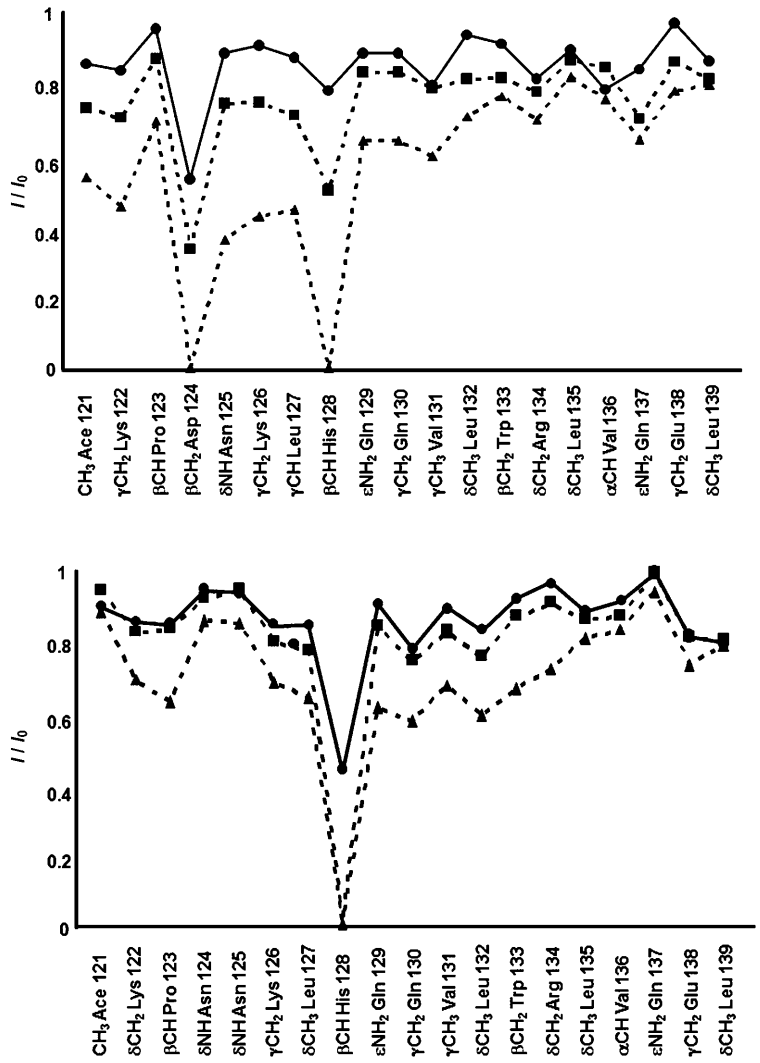

Figure 7. I/I_0 profiles of the ^{1}H signals of A) hDpl(122–139) and B) hDpl(122–139)D124N at 1×10^{-3} mol dm^{-3} and pH 5.5 in the presence of 0.05 (●), 0.1 (■) and 0.3 equivalents (▲) of Cu^{II}.

$\lambda = 290$–310 nm in the CD spectrum provides unambiguous proof of the contemporary existence of Cu–N(imidazole) and Cu–N(amide) bonds in this species, whereas the relatively high ε value reflects a distorted coordination environment. The EPR parameters ($g_{\parallel}=2.275$ and $A_{\parallel}=175\times10^{-4}$ cm^{-1}) obtained at pH 7 (Figure 8A) suggest an apical disposition of the carboxylate group. In fact, the hyperfine constant value confirms a slight distortion of the coordination plane in comparison to a classic six-membered chelate ring involving imidazole and amide nitrogen donor atoms.[29]

It is interesting to note that the EPR spectroscopic parameters found for the $[CuLH]^+$ complex with hDpl(122–139), which were not determined for shorter hDpl(122–130), are similar to those reported for the copper(II) complex species with the whole protein in the pH range of 5 to 6 (D2:[20] $g_{\parallel}=2.280$ and $A_{\parallel}=174\times10^{-4}$ cm^{-1}[20]). The $[CuLH]^{2+}$ complex of hDpl(122–139)D124N only forms in small quantities and consequently its spectral parameters cannot be determined, but this difference with respect to hDpl(122–139) is further proof of the involvement of the carboxylate group in copper(II) binding. Evidently, this coordination mode (N_{Im}, N^-, COO^-, $2H_2O$) is favored by the α-helical conformation of hDpl(122–139).

Further deprotonation of an amide nitrogen atom occurs during the formation of the minor species [CuL], which corresponds to $[CuLH_{-2}(H_2)]$. Due to its low concentration, we resorted to difference spectra obtained at pH 7 and 8 to determine the EPR spectroscopic parameters for this species ($g_{\parallel}=2.264$ and $A_{\parallel}=182\times10^{-4}$ cm^{-1}; see Figure 8A). These values are consistent with a 3N1O (one imidazole and two amide nitrogen atoms) coordination environment. It is worth noting that the EPR parameters of this minor complex species are similar to those attributed to a second copper binding site with low affinity in the whole protein (D4:[20] $g_{\parallel}=2.260$ and $A_{\parallel}=187\times10^{-4}$ cm^{-1}[20]).

Conversely, $[CuL]^+$ is the prevailing complex with hDpl(122–139)D124N in the pH range of 7 to 8. The spectroscopic parameters clearly indicate a 3N1O coordination environment with one imidazole and two amide nitrogen atoms coordinated to the metal ion; the lysine residues remain protonated, and the $[CuL]^+$ corresponds to $[CuLH_{-2}(H_2)]^+$. The EPR parameters obtained for this complex species (Figure 8B) are very similar both to those obtained for the analogous complex with shorter peptide fragments hDpl(122–130) and hDpl(122–139)D124N.[22] Upon increasing the pH, a further deprotonation of an amide nitrogen of hDpl(122–139) results in the formation of $[CuLH_{-1}]^-$, which is the prevailing metal complex at pH values higher than 7.4 ($K_d=1.3\times10^{-5}$ mol dm^{-3}). It is interesting to note that the pK_{lh} values of the successive amide deprotonation steps do not follow the expected trend of a cooperative process.[31] The blueshift of the UV/Vis λ_{max} and the increase of the $N^-\rightarrow Cu^{II}$ charge-transfer band at $\lambda=310$ nm in the CD spectra clearly indicate a N_{Im}, $3N^-$ coordination mode; the two lysyl ε-amino groups are still protonated, thus $[CuLH_{-1}]^-$ corresponds to $[CuLH_{-3}(H_2)]^-$. The analogous copper(II) complex with mutated peptide hDpl-

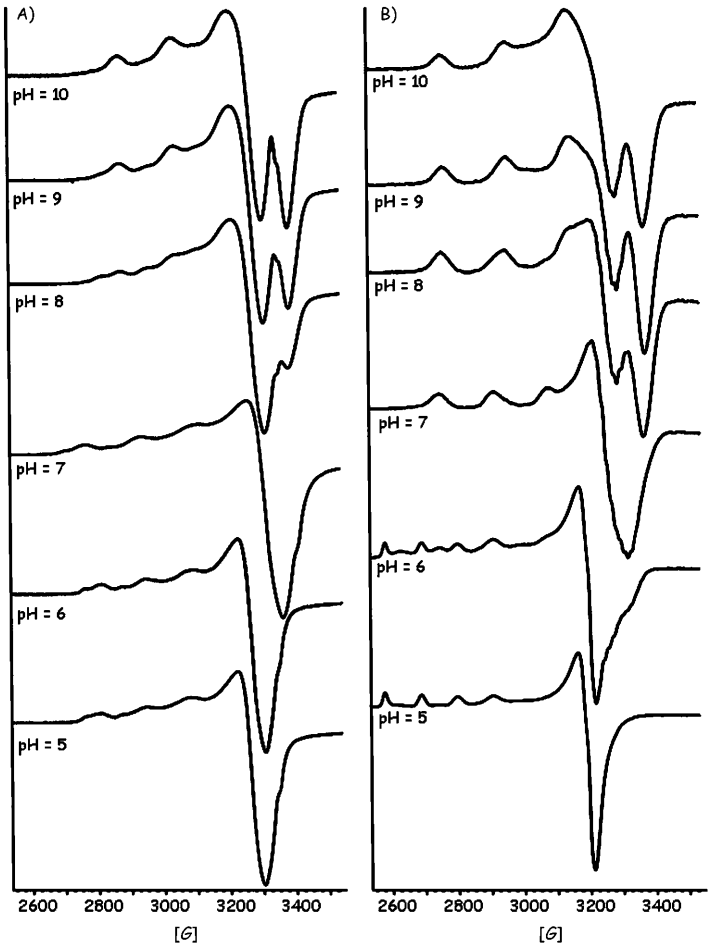

Figure 8. Frozen-solution EPR spectra at 150 K and different pH values of A) Cu–hDpl(122–139); B) Cu–hDpl(122–139)D124N. ($[L]=[Cu^{2+}]=1\times10^{-3}$ mol dm^{-3}).

(122–139)D124N displays the same spectroscopic parameters; this confirms that the carboxylate group is no longer directly involved in the metal binding. The Hamiltonian parameters of $[CuLH_{-1}]^-$ are identical to those reported for the shorter peptide fragments,[22] and are similar to those of the main copper complex species reported for the hDpl protein in the pH range 7–8 (D3:[20] $g_{\parallel}=2.205$ and $A_{\parallel}=197\times10^{-4}$ cm^{-1}[20]). This overlap of EPR spectroscopy data suggests that the coordination mode of the copper(II) bound to the whole protein involves the same four nitrogen atoms (one imidazole and three amide nitrogen atoms) experienced by the metal ion in the complex with the peptide model. The thermodynamic data indicate that the amide deprotonation takes place towards the N-terminal region of the peptide, so to involve the residues His, Leu, and Lys in copper(II) binding. The His and Leu residues are located at the beginning of the α-helix region in the peptide as well as in the whole protein, whereas the Lys residue is part of the loop region. This finding might explain why the α-helix is not abolished upon copper(II) coordination and why the corresponding complex species with the shorter hDpl(122–130) displayed similar spectroscopic parameters to those obtained for the structured hDpl(122–139). Upon increasing the pH, two other deprotonation processes occur. However, the lack of any spectral changes above pH 9 indicates the involvement of the two lysyl ammonium group so that both $[CuLH_{-2}]^{2-}$ and $[CuLH_{-3}]^{3-}$ have the same (N_{Im}, $3N^-$) binding mode of the $[CuLH_{-1}]^-$ complex species.

Copper(II) binding affinity—Comparison of different regions of PrP^C with the binding site domain of hDpl: It is worth noting that a strong interaction between PrP^C and Dpl has recently been demonstrated;[32] this also indicates that, unlike full-length PrP^C, the N-terminally deleted PrP^C is incapable of rescuing Dpl-induced degeneration.[12,13] Furthermore, it has been shown by surface plasmon resonance measurements that the N-terminal-truncated isoform of PrP^C binds to Dpl with less efficacy.[32] Similarly, another recent paper[33] not only reported that Dpl-induced cytotoxicity was antagonized by the presence of full-length wild-type PrP, but also showed that the N-terminal fragment of PrP^C was responsible for the protective activity; it is worth noting that this effect increased in the presence of copper ions. In fact, this region encompasses the octarepeat domain that has been shown to bind copper(II).[18] These studies and our results suggest that the competition between the PrP^C and Dpl proteins for this metal ion could arise from the same causes as the molecular events underlying PrP-mediated rescue of Dpl neurotoxicity. The distribution diagrams reported in Figures 9 and 10 were used to compare the metal binding affinity of the hDpl(122–139) with that of the peptide encompassing a single octarepeat (PrP^C 60–67)[34] and the whole tetraoctarepeat domain (PrP^C 60–91)[35] of the prion.

Figure 9A clearly shows that hDpl(122–139) is able to bind a single copper(II) ion more tightly than an octarepeat peptide. This behavior is more evident in the acidic pH range; upon increasing the pH, the copper(II) is distributed among the prion octarepeat species, [CuL′H-2] (L′ = octarepeat peptide), and the two hDpl(122–139) complexes that together represent about a double amount of copper(II) complex species at pH 7.4. In the presence of an excess of the hDpl peptide fragment, the competition results are more favorable towards doppel than prion (Figure 9B). On the contrary, the tetraoctarepeat peptide is a stronger ligand for the metal ion than hDpl(122–139) (Figure 10A). Upon increasing the ratio of hDpl/tetraoctarepeat (Figure 10B), the distribution diagram shows the preference of copper(II) for doppel in comparison to prion over an acidic pH range. In addition, being aware of the notion that the copper-binding sites within the α-helical domain of a cellular prion protein have precedent from studies of PrP^C,[36,37] the comparison was extended to the affinity of copper(II) to the Dpl third helix and the PrP^C second helix. Figure 11 shows the distribution diagram obtained for copper(II) complexes with Dpl-(122–139) and the peptide fragment PrP^C(184–188) blocked at the C and N terminus, which has been shown to be a reliable model for the interaction between metals and the helix II domain of prion.[38] The diagram shows that at acidic pH

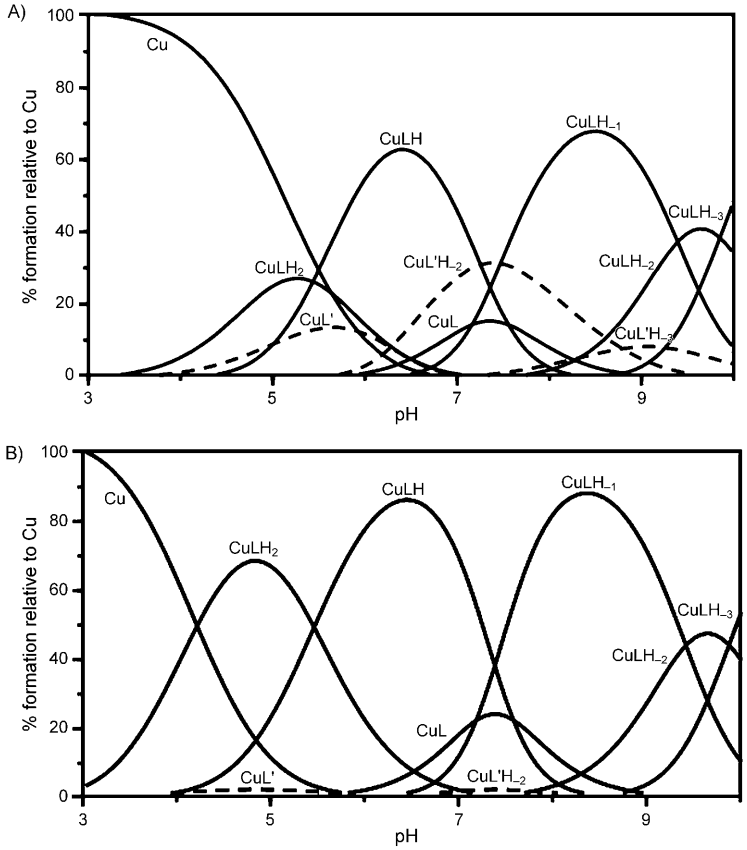

Figure 9. Species distribution diagram for the Cu^{II}–hDpl(122–139) (L, ——) and Cu^{II}–PrP^C(60–67) (L′, – – –; data from ref. [34]) complexes formed at Cu/L/L′ molar ratios of 1:1:1 (A) and 1:10:1 (B).

values, hDpl(122–139) binds copper(II) more tightly than PrP^C(184–188), whereas at physiological pH the affinity is inverted and 60% of the copper is bound to PrP^C(184–188).

Conclusion

hDpl(122–139), which encompasses the third helix of doppel, mimics in a complete way the interaction of copper(II) with the whole protein. In fact, the EPR parameters previously attributed to different copper(II) binding sites of hDpl[20] are nearly the same as those obtained for the metal complexes with hDpl(122–139). Our results permit us to describe the binding ability of doppel in terms of a single species with a given stability constant, and show the maximum percentage of formation at different pH values and in specific coordination environments. This finding is different from that displayed by the shorter peptide fragment previously investigated,[22] and it stresses the role played by the conformational properties of the protein domain on copper(II) binding. The helical structure of the Dpl peptide fragment is preserved in the copper(II) complexes, as shown by the CD and NMR spectroscopy data reported herein. Furthermore, comparison of hDpl(122–139) secondary structure with that of the single-point-mutated hDpl(122–139)D124N gave evidence for the significant role of the aspartic residue on the helical conformation of the peptide. Asp124 not only drives the peptide conformation, but also stabilizes the macrochelate formation in metal complexes $[CuLH_2]^{2+}$ and $[CuLH]^+$, which are the prevailing species formed at pH values of up to 7. Upon increasing the pH, the predominant complex species is $[CuLH_{-1}]^-$, and its EPR parameters correspond to those of the main copper(II) complex species reported for the whole protein.[20]

A plausible mechanism of doppel-mediated neurodegeneration has been recently proposed;[32] in the same study, a strong interaction between PrP^C and Dpl was demonstrated, which indicates an intriguing, plausible molecular mechanism for their biological antagonism. Interestingly, addition of copper increases the antagonizing effect of the N-terminal region of PrP^C.[33] Our results show that the different affinities of doppel and prion for copper is tuned by pH values. The favored binding of copper(II) with hDpl(122–139) in the acidic pH range can be attributed to the aspartic acid binding that is present in the copper(II) coordination environment of $[CuLH_2]^{2+}$ and $[CuLH]^+$. On increasing the pH, amide deprotonation occurs and the difference between the stability constants of the metal-ion complexes of the octarepeat peptide and those displayed by the copper(II) com-

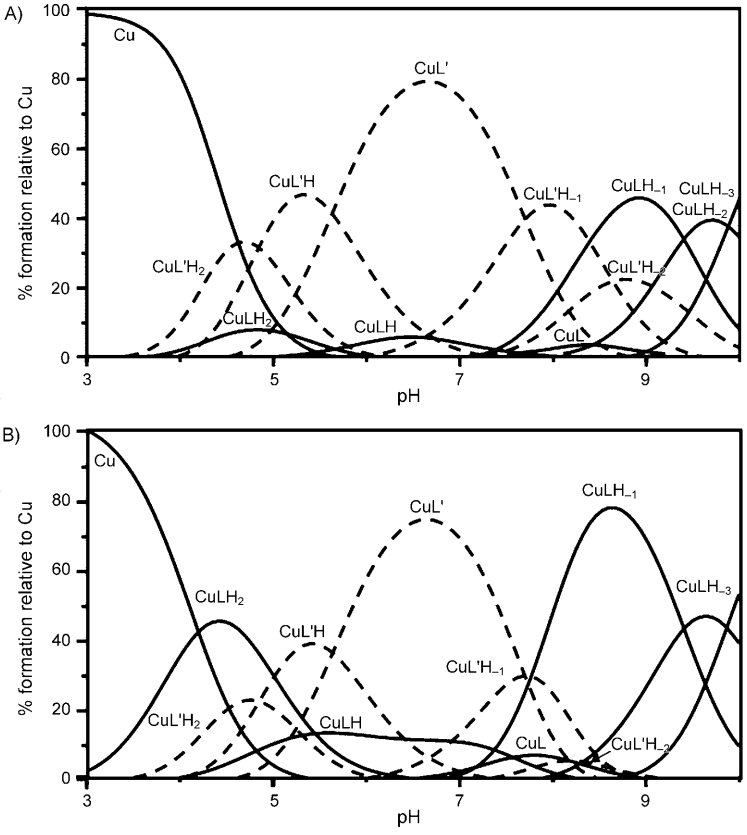

Figure 10. Species distribution diagram for the Cu^{II}–hDpl(122–139) (L, ——) and Cu^{II}–PrP^C(60–91) (L′, – – –; data from ref. [35]) complexes formed at Cu/L/L′ molar ratios of 1:1:1 (A) and 1:10:1 (B).

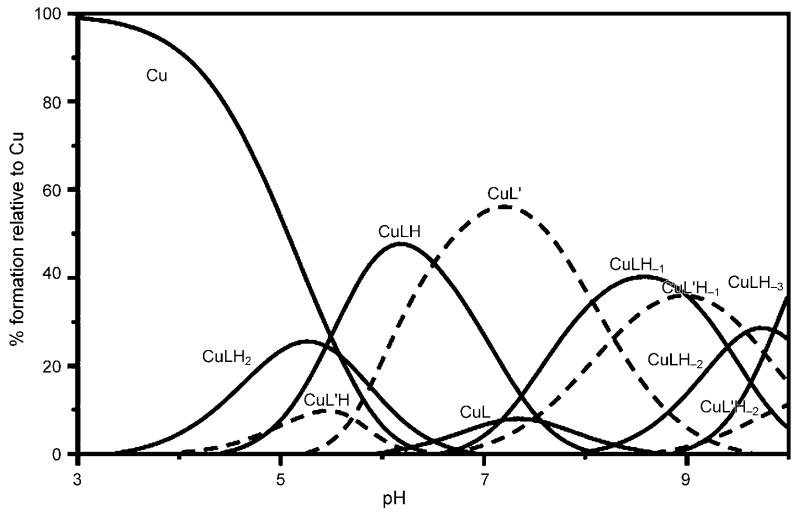

Figure 11. Species distribution diagram for the Cu^{II}–hDpl(122–139) (L, ——) and Cu^{II}–PrP^{C}(184–188) (L′, – – –; data from ref. [38]) complexes formed at a molar ratio of 1:1:1.

plexes of the doppel peptide decreases. The Asp residue also plays a favorable role over the acidic pH range when the stability of copper(II) complexes with doppel is compared with metal complexes of the tetraoctarepeat peptide. At physiological pH values, the tetraoctarepeat forms a macrochelate 4N complex ($4N_{Im}$ of the four histidine residues) that is more stable than the 3N complex(N_{Im}, $2N^-$ of the deprotonated amides) formed by the α-helical domain of doppel. We are tempted to speculate that the different coordination environments of the various copper(II) species can influence the orientation of the amino acid residues responsible of the interaction between doppel and prion proteins and that this interaction can change as function of pH values.

Experimental Section

Materials: All *N*-fluorenylmethoxycarbonyl (Fmoc)-protected amino-acids and 2-(1-H-benzotriazole-1-yl)-1,1,3,3-tetramethyluronium tetrafluoroborate (TBTU) were obtained from Novabiochem (Laufelfingen, Switzerland). Fmoc-PAL-PEG resin, *N*,*N*-diisopropyl-ethylamine (DIEA), *N*,*N*-dimethylformamide (DMF; peptide synthesis grade), and 20% piperidine in DMF were obtained from Applied Biosystems (Foster City, CA, USA). *N*-hydroxybenzotriazole (HOBT), triisopropylsilane (TIS), and trifluoroacetic acid (TFA) were purchased from Sigma–Aldrich. All the other chemicals were of the highest available grade and were used without further purification.

Peptide synthesis and purification: Peptides hDpl(122–139) and hDpl-(122–139)D124N were synthesized in the N-acetylated and C-amidated form to avoid end-group effects and more properly mimic their protein-fragment character. They were assembled by using the solid-phase peptide synthesis strategy by using a Pioneer Peptide Synthesizer. All amino acid residues were added according to the TBTU/HOBT/DIEA activation method for Fmoc chemistry on Fmoc-PAL-PEG resin (substitution: 0.22 mmol g^{-1}, synthesis scale: 0.33 mmol, resin: 1.5 g). Other experimental details have already been reported.[22] The peptides were purified by using preparative reversed-phase high-performance liquid chromatography (rp-HPLC). Purification was performed by using a Varian Prep-Star 200 model SD-1 chromatography system equipped with a Prostar photodiode array detector with detection at 222 nm. The peptides were eluted with solvent A (0.1% TFA in H_2O) and B (0.1% TFA in MeCN) on a Vydac C_{18} 250×22 mm (300 Å pore size, 10–15 mm particle size) column at flow rate of 10 mL min^{-1}. Analytical rp-HPLC analyses were performed by using a Waters 1525 instrument, equipped with a Waters 2996 photodiode array detector with detection at $\lambda = 222$ nm. The peptide samples were analyzed by using gradient elution with solvents A and B on a Vydac C_{18} 250×4.6 mm (300 Å pore size, 5 mm particle size) column at a flow rate of 1 mL min^{-1}. The peptides were eluted according to the following protocol: an isocratic gradient in 5% B from 0 to 8 min, followed by a linear gradient of 5 to 25% B over 25 min, and finally an isocratic gradient in 25% B from 25 to 40 min. They were characterized by means of ESI-MS.

hDpl(122–139) (Ac-KPDNKLHQQVLWRLVQEL-NH_2): Yield = 50%, R_t = 35.60 min; ESI-MS: *m*/*z* calcd for $C_{104}H_{169}N_{31}O_{27}$: 2285.68; found: 1143.9 $[M+2H]^{2+}$, 762.9$[M+3H]^{3+}$.

hDpl(122–139)D124N (Ac-KPNNKLHQQVLWRLVQEL-NH_2): Yield = 55%, R_t = 36.80 min; ESI-MS: *m*/*z* calcd for $C_{104}H_{170}N_{32}O_{26}$: 2284.69; found: 1143.5 $[M+2H]^{2+}$, 762.6 $[M+3H]^{3+}$.

Potentiometric and UV/Vis titrations: Potentiometric titrations were performed by using a computer-controlled Metrohm digital pH meter (model 654) and Hamilton digital dispenser (mod. 665). The titration cell (2.5 mL) was thermostated at 298.0±0.2 K and all solutions were kept under an argon atmosphere, which was bubbled through another solution under the same conditions of ionic strength and temperature. A KOH solution was added by using a Hamilton burette equipped with a 1 cm^3 syringe. The combined microelectrode was calibrated on the pH = $-\log[H^+]$ scale by titrating HNO_3 with CO_2 free base. The ionic strength of all solutions was adjusted to 0.1 mol dm^{-3} (KNO_3). The concentrations of HNO_3 and KOH stock solutions were determined by titrations with tris(hydroxymethyl)aminomethane and potassium hydrogen phthalate, respectively. All solutions were prepared with double-distilled H_2O. The analytical concentrations of peptides were varied from 1×10^{-3}–3.5×10^{-3} mol dm^{-3}. Different metal-to-ligand ratios (between 2.1:1 and 1:1) were employed. Stability constants for proton complexes were calculated from two or three peptide titrations carried out over the pH range of 2.3–11. Duplicate or triplicate titrations were performed to determine the copper(II) complex stability constants in the pH range of 3–11. Other details were as previously reported.[39] All potentiometric data were handled by using the HYPERQUAD program,[40] which minimizes the error-square sum of the differences between measured and calculated electrode potentials. Distribution diagrams were calculated by using the Hyss program.[41] Errors in stability constant values are reported as the standard deviation of three experiments. The formation reaction equilibria of the ligands with protons and copper(II) ions are given in Equation (1):

$$m\mathrm{Cu} + l\mathrm{L} + h\mathrm{H} \rightleftharpoons \mathrm{Cu}_m\mathrm{L}_l\mathrm{H}_h \quad (1)$$

in which L are the peptides under study. The stability constant β_{mlh} is defined in Equation (2):

$$\beta_{mlh} = [\mathrm{Cu}_m\mathrm{L}_l\mathrm{H}_h]/[\mathrm{Cu}]^m \cdot [\mathrm{L}]^l \cdot [\mathrm{H}]^h \quad (2)$$

Combined spectroscopic and potentiometric titrations were performed in a 3 mL quartz cuvette with a 1 cm path length to get the spectrum in the

visible region at each pH value simultaneously. The optical spectra were recorded by using an Agilent 8453 spectrophotometer. These experiments were replicated at least three times for each peptide. Both spectroscopic and potentiometric data were processed by using the HYPERQUAD program.[40]

CD measurements: CD spectra of the peptides and their copper(II) complexes were recorded by using a JASCO 810 spectropolarimeter at a scan rate of 50 nm min^{-1} and a resolution of 0.1 nm. The pathlength was 1 cm, in the $\lambda = 190$–800 nm range. The spectra were recorded as an average of 10 or 20 scans. The CD instrument was calibrated with ammonium(+)-camphor-10-sulfonate. The deconvolution of the spectra were carried out by using the Circular Dichroism Neural Network (CDNN) program by using the complex spectrum database.[24]

EPR measurements: A Bruker Elexsys E500 CW-EPR spectrometer driven by a PC running the Xepr program under the Linux operating system and equipped with a Super X-band microwave bridge operating at 9.3–9.5 GHz and a SHQE cavity was used throughout this work. All frozen-solution EPR spectra of the copper(II) complexes were recorded at 150 K by means of a variable-temperature apparatus. $^{63}Cu(NO_3)_2$ (0.05 mol dm^{-3}) in dilute nitric acid was used as the source of copper(II) to avoid overlapping spectra from the ^{65}Cu isotope. Copper(II) complexes in a concentration range of 4×10^{-4}–1×10^{-3} mol dm^{-3} and at different metal–ligand molar ratios were prepared in water by varying the pH by the addition of NaOH. To obtain a good-quality glass upon freezing, aqueous solutions containing a small amount of MeOH (not exceeding 10%) were used. The instrumental settings for EPR spectrum recording were as follows: number of scans 1–5; microwave frequency 9.344–9.376 GHz; modulation frequency 100 kHz; modulation amplitude 0.2–0.6 mT; time constant 164–327 ms; sweep time 2.8 min; microwave power 20–40 mW; receiver gain 1×10^4–2×10^5.

NMR spectroscopy measurements: All the experiments were carried out at 500 MHz by using a Varian UNITY 500 spectrometer. Spectra were processed by using the Varian VnmrJ and XEASY[42] software. Sample solutions (about 1.2 mM) were prepared in H_2O/D_2O 90:10 (v/v) or neat D_2O. Deuterated D_2O (99.9% relative isotopic abundance) was purchased from Cambridge Isotope Laboratories. NMR spectra for the three-dimensional structure determination were collected at 300 K and referenced to external TMS ($\delta = 0$ ppm). The dependence of the amide chemical shifts on the temperature was observed between 300 and 311 K. One- (1D) and two-dimensional (2D) spectra were accumulated with a spectral width of 5800 Hz. 2D experiments DQFCOSY,[43] TOCSY,[44] ROESY,[45] and NOESY[46] were recorded in the phase-sensitive mode by using the States–Haberkorn method. Water suppression was achieved by using the DPFGSE sequence.[47] TOCSY, NOESY, and ROESY spectra were acquired with mixing times of 70, 250, and 150 ms, respectively. Typically, 64 transients of 4 K data points were collected for each of the 256 increments; the data were zero-filled to 1 K in ω_1. Squared shifted sine-bell functions were applied in both dimensions prior to Fourier transformation and baseline correction. NMR spectroscopy experiments for hDpl(122–139) and hDpl(122–139)D124N peptide structure determination were carried out at dissolution pH (i.e., 4.0 for hDpl(122–139) and 5.1 for hDpl(122–139)D124N). ^{1}H resonance assignment was obtained by using a standard protocol; the ^{1}H assignment for both peptides was also performed at pH 5.5. Proton chemical shifts, ^3J(HN,Hα) scalar coupling, and $\Delta\delta/\Delta T$ at dissolution and at pH 5.5 have been submitted to the BMRB; these data can be found under accession numbers 16522 (hDpl-(122–139)) and 16511 (hDpl(122–139)D124N). To analyze the copper coordination features of both peptides, the samples were titrated with different aliquots of a stock solution of $CuSO_4$ (3.5×10^{-3} mol dm^{-3} in H_2O/D_2O (90:10)) to give molar ratios of the paramagnetic metal relative to peptide of 0.05, 0.1, 0.3, and 0.5 equiv. The pH value of the peptide solutions was adjusted to 5.5 by using HCl and NaOH. For each point of the copper titration, one-dimensional ^{1}H NMR spectra were acquired (300 K); the amide and side-chain protons affected during Cu^{II} titration were identified by comparing their intensities (I) with those of the same peak (I_0) in the dataset of the metal-free samples. To obtain intensity profiles, the I/I_0 ratios of the nonoverlapping peaks of hDpl(122–139) and hDpl(122–139)D124N were plotted as a function of the peptide sequences. Pulse field gradient (PFG) diffusion measurements with the PG-SLED (pulse gradient-stimulated echo longitudinal encode–decode) sequence[48] enabled us to obtain D_{trans}, which is proportional to the decay rate of the NMR signal attenuation as a function of gradient strength.[49] Each diffusion data set contained a series of 13 one-dimensional ^{1}H spectra with gradient strength from 0.5 to 30 G cm^{-1}. Data processing for obtaining of the translational diffusion coefficient D_{trans} were obtained by DOSY package of the VNMRJ software.

Structure calculations: Experimental distance restraints for structure calculations were derived from the cross-peak intensities in the NOESY and ROESY spectra for hDpl(122–139) and hDpl(122–139)D124N, respectively, because the NOESY experiments were scarcely informative for hDpl(122–139). The cross-peaks were manually integrated by using the XEASY software[42] and converted to upper distance constraints according to an inverse sixth-power peak volume-to-distance relationship for the backbone and to an inverse fourth-power function for side-chains, by using the CALIBA module of the CYANA program.[50] Distance constraints together with the obtained scalar coupling constants were then used by the GRIDSEARCH module, implemented in CYANA, to generate a set of allowable dihedral angles. Structure calculations, which used the torsion angle dynamics protocol of CYANA, were then started from 100 randomized conformers. The 20 conformers with the lowest CYANA target functions were further refined in vacuo by means of unrestrained energy minimization by using the GROMOS 96[51] force field with the program SPDB viewer.[52] Several cycles of steepest descent were repeated until the energy difference between two successive steps was less than 10^{-3} kJ mol^{-1}. Structural analysis was performed by using the program MOLMOL.[53]

Acknowledgements

This work was supported by MIUR (PRIN 2006033492 and FIRB RBNEO3K83). E. Rizzarelli and D. La Mendola wish to thank the Short-Term Mobility Program of National Council of Research (CNR-Rome).

[1] K. Peoc'h, C. Serres, Y. Frobert, C. Martin, S. Lehmann, S. Chasseigneaux, V. Sazdovitch, J. Grassi, P. Jouannet, J. M. Launay, J. L. Laplanche, *J. Biol. Chem.* **2002**, *277*, 43071–43078.
[2] A. Li, S. Sakaguchi, K. Shigematsu, R. Atarashi, B. C. Roy, R. Nakaoke, K. Arima, N. Okimura, J. Kopacek, S. Katamine, *Am. J. Pathol.* **2000**, *157*, 1447–1452.
[3] A. Behrens, N. Genoud, H. Naumann, T. Rulicke, F. Janett, F. L. Heppner, B. Ledermann, A. Aguzzi, *EMBO J.* **2002**, *21*, 3652–3658.
[4] S. Sakaguchi, S. Katamine, N. Nishida, R. Moriuchi, K. Shigematsu, T. Sugimoto, A. Nakatani, Y. Kataoka, T. Houtani, S. Shirabe, H. Okada, S. Hasegawa, T. Miyamoto, T. Noda, *Nature* **1996**, *380*, 528–531.
[5] R. C. Moore, I. Y. Lee, G. L. Silverman, P. M. Harrison, R. Strome, C. Heinrich, A. Karunaratne, S. H. Pasternak, M. A. Chishti, Y. Liang, P. Mastrangelo, K. Wang, A. F. Smit, S. Katamine, G. A. Carlson, F. E. Cohen, S. B. Prusiner, D. W. Melton, P. Trembley, L. E. Hood, D. Westaway, *J. Mol. Biol.* **1999**, *292*, 797–817.
[6] Y. Shaked, H. Rosenmann, G. Talmor, R. Gabizon, *J. Biol. Chem.* **1999**, *274*, 32153–32158.
[7] T. Lührs, R. Riek, P. Gtert, K. Wutrich, *J. Mol. Biol.* **2003**, *326*, 1549–1557.
[8] D. Rossi, A. Cozzio, E. Flechsig, M. A. Klein, T. Rulicke, A. Aguzzi, C. Weissmann, *EMBO J.* **2001**, *20*, 694–702.
[9] L. Anderson, D. Rossi, J. Linehan, S. Brandner, C. Weissmann, *Proc. Natl. Acad. Sci. USA* **2004**, *101*, 3644–3649.
[10] I. Radovanovic, N. Braun, O. T. Giger, K. Mertz, G. Miele, M. Prinz, B. Navarro, A. Aguzzi, *J. Neurosci.* **2005**, *25*, 4879–4888.

[11] H. Mo, R. C. Moore, F. E. Cohen, D. Westaway, S. B. Prusiner, P. E. Wright, H. J. Dyson, *Proc. Natl. Acad. Sci. USA* **2001**, *98*, 2352–2357.
[12] J. C. Watts, D. Westaway, *Biochim. Biophys. Acta Mol. Basis Dis.* **2007**, *1772*, 654–672.
[13] K. Qin, M. O'Donnel, R. Y. Zhao, *Neuroscience* **2006**, *141*, 1–8.
[14] D. Yoshikawa, N. Yamaguchi, D. Ishibashi, H. Yamanaka, N. Okimura, Y. Yamaguchi, T. Mori, H. Miyata, K. Shigematsu, S. Ketamine, S. Sakaguchi, *J. Biol. Chem.* **2008**, *283*, 24202–24211.
[15] A. Behrens, *Br. Med. Bull.* **2003**, *66*, 35–42.
[16] D. R. Brown, K. Qin, J. W. Herms, A. Madlung, J. Manson, R. Stromer, P. E. Fraser, T. Kruck, A. von Bohlens, W. Schulz-Schaeffer, A. Giese, D. Westaway, H. Kretzschmar, *Nature* **1997**, *390*, 662–687.
[17] G. L. Millhauser, *Ann. Pharm. Belg.* **2007**, *58*, 299–320.
[18] R. P. Bonomo, D. La Mendola, G. Pappalardo, E. Rizzarelli, I. Sovago in *Recent Development in Bioinorganic Chemistry: Metal Complexes of Bioactive Molecules* (Ed.: M. Saviano) Transworld Research Network, Kerala, pp. 133–160, **2006**.
[19] K. Qin, J. Coomaraswamy, P. Mastrangelo, Y. Yang, S. Lugowski, C. Petromilli, S. B. Prusiner, P. E. Fraser, J. M. Goldberg, A. Chakrabartty, D. Westaway, *J. Biol. Chem.* **2003**, *278*, 8888–8896.
[20] G. M. Cereghetti, A. Negro, M. L. Massimino, M. C. Sorgato, S. Van Doorslaer, *J. Biol. Chem.* **2004**, *279*, 36497–36503.
[21] B. Drisaldi, J. Coomaraswamy, P. Mastrangelo, B. Strome, J. Yang, J. C. Watts, M. A. Chishti, M. Marvi, O. Windl, R. Ahrens, F. Major, M. S. Sy, H. Kretzschmar, P. E. Fraser, H. T. J. Mount, D. Westaway, *J. Biol. Chem.* **2004**, *279*, 55443–55454.
[22] D. La Mendola, A. Magrì, Ö. Hansson, R. P. Bonomo, E. Rizzarelli, *J. Inorg. Biochem.* **2009**, *103*, 758–765.
[23] A. J. Nicoll, D. J. Milelr, K. Futterer, R. Ravelli, R. K. Allemann, *J. Am. Chem. Soc.* **2006**, *128*, 9187–9193.
[24] G. Böhm, R. Muhr, R. Jaenicke, *Protein Eng.* **1992**, *5*, 191–195.
[25] A. Chakrabartty, T. Kortemme, S. Padmanabhan, R. L. Baldwin, *Biochemistry* **1993**, *32*, 5560–5565.
[26] R. W. Woody A. K. Dunker in *Circular Dichroism and the Conformational Analysis of Biomolecules* (Ed.: G. D. Fasman) Plenum Press, New York, **1996**, pp. 109–157.
[27] C. Kállay, K. Varnagy, G. Micera, D. Sanna, I. Sovago, *J. Inorg. Biochem.* **2005**, *99*, 1514–1525.
[28] B. Bóka, A. Myari, I. Sovago, N. Hadjiliadis, *J. Inorg Biochem.* **2004**, *98*, 113–122.
[29] D. La Mendola, R. P. Bonomo, G. Impellizzeri, G. Maccarrone, G. Pappalardo, E. Rizzarelli, A. Pietropaolo, V. Zito, *J. Biol. Inorg. Chem.* **2005**, *10*, 463–475.
[30] W. Guangshun, A. Peterkofsky, P. A. Keifer, X. Li, *Protein Sci.* **2005**, *14*, 1082–1090.
[31] K. Osz, I. Sovago, *Dalton Trans.* **2006**, 3841–3854.
[32] S. Benvegnù, D. Franciotta, J. Sussman, A. Bachi, E. Cardini, P. Torreri, C. Govaerts, S. Pizzo, G. Legname, *PLos One* **2009**, *4*, e5968.
[33] P. Li, C. Dong, Y. Lei, B. Shan, X. Xiao, H. Jiang, X. Wang, C. Gao, Q. Shi, K. Xu, C. Tian, J. Han, X. Dong, *Acta Biochim. Biophys. Sin.* **2009**, *41*, 42–53.
[34] R. P. Bonomo, V. Cucinotta, A. Giuffrida, G. Impellizzeri, A. Magrì, G. Pappalardo, E. Rizzarelli, A. M. Santoro, G. Tabbì, L. I. Vagliasindi, *Dalton Trans.* **2005**, 150–158.
[35] D. Valensin, M. Luczkowski, F. M. Mancini, A. Legowska, E. Gaggelli, G. Valensin, K. Rolka, H. Kozlowski, *Dalton Trans.* **2004**, 1284–1293.
[36] G. M. Cereghetti, A. Schweiger, R. Glockshuber, S. Van Doorslaer, *Biophys. J.* **2001**, *81*, 516–525.
[37] D. R. Brown, V. Guantieri, G. Grasso, G. Impellizzeri, G. Pappalardo, E. Rizzarelli, *J. Inorg. Biochem.* **2004**, *98*, 133–143.
[38] D. Grasso, G. Grasso, V. Guantieri, G. Impellizzeri, C. La Rosa, D. Milardi, G. Micera, K. Osz, G. Pappalardo, E. Rizzarelli, D. Sanna, I. Sovago, *Chem. Eur. J.* **2006**, *12*, 537–547.
[39] R. P. Bonomo, R. Calì, V. Cucinotta, G. Impellizzeri, E. Rizzarelli, *Inorg. Chem.* **1986**, *25*, 1641–1646.
[40] P. Gans, A. Sabatini, A. Vacca, *Talanta* **1996**, *43*, 1739–1753.
[41] L. Alderighi, P. Gans, A. Ienco, D. Peters, A. Sabatini, A. Vacca, *Coord. Chem. Rev.* **1999**, *184*, 311–318.
[42] C. Bartels, T. Xia, M. Billeter, P. Güntert, K. Wüthrich, *J. Biomol. NMR* **1995**, *6*, 1–10.
[43] M. Rance, O. W. Sørensen, G. Bodenhausen, G. Wagner, R. R. Ernst, K. Wüthrich, *Biochem. Biophys. Res. Commun.* **1983**, *117*, 479–485.
[44] L. Braunschweiler, R. R. Ernst, *J. Magn. Reson.* **1983**, *53*, 521–528.
[45] C. Griesinger, R. R. Ernst, *J. Magn. Reson.* **1987**, *75*, 261–271.
[46] A. Kumar, R. R. Ernst, K. Wüthrich, *Biochem. Biophys. Res. Commun.* **1980**, *95*, 1–6.
[47] T. L. Hwang, A. J. Shaka, *J. Magn. Reson. Ser. A* **1995**, *112*, 275–279.
[48] E. O. Stejskal, J. E. Tanner, *J. Chem. Phys.* **1965**, *42*, 288–292.
[49] C. Chatterjee, B. Majumder, C. Mukhopadhyay, *J. Phys. Chem. B* **2004**, *108*, 7430–7436.
[50] T. Herrmann, P. Güntert, K. Wüthrich, *J. Mol. Biol.* **2002**, *319*, 209–227.
[51] W. F. Gunsteren, S, R. Billeter, A. A. Eising, P. H. Hünenberger, P. Krüger A. E. Mark, W. R. P. Scott, I. G. Tironi, Biomolecular simulation: the GROMOS96 manual and user guide (BIOMOs), **1996**.
[52] N. Guex, M. C. Peitsch, *Electrophoresis* **1997**, *18*, 2714–2723.
[53] R. Koradi, M. Billeter, K. Wüthrich, *J. Mol. Graph.* **1996**, *14*, 51–55.

Received: August 31, 2009
Revised: March 25, 2010
Published online: April 21, 2010

